

INFLUENCE OF LASER BEAM WELDING PARAMETERS ON LOCAL MECHANICAL PROPERTIES OF DUPLEX STAINLESS STEEL JOINTS

PAVEL KOVAČÓCY^{a,*}, MAROŠ MARTINKOVIČ^a, BEÁTA ŠIMEKOVÁ^a,
MARTIN HNILICA^a, INGRID KOVAŘÍKOVÁ^b, JIŘÍ MACHÁČEK^b, MICHAL KRBAŤA^b

^a Slovak University of Technology in Bratislava, Faculty of Materials Science and Technology in Trnava,
J. Bottu 25, 91724 Trnava, Slovak Republic

^b Alexander Dubček University of Trenčín, Faculty of Special Technology, Ku kyselke 469, 91106 Trenčín,
Slovak Republic

* corresponding author: pavel.kovacocy@stuba.sk

ABSTRACT. Duplex stainless steels (DSS) are dual-phase alloys consisting of austenitic and ferritic phases in the microstructure. DSS provide an ideal compromise between mechanical properties and corrosion resistance. Welding of DSS leads to a change in the ferrite/austenite ratio in the microstructure and to degradation of the properties of the weld joints. Therefore, it is very important to control the microstructure of the weld joint directly during the welding process. An innovative method of laser welding applying a dual beam was used. By spreading the energy of the laser beam over two spots, additional heat is introduced into the weld, which ensures a slowdown in the cooling rate of the DSS and possibly ensures the desired ratio of ferrite and austenite in the microstructure. The influence of laser welding parameters and energy distribution of the dual beam on the fusion zone (FZ) geometry, resulting microstructure and mechanical properties of the weld joints was monitored. The tensile and shear strength was measured. The coefficient of proportionality between shear and tensile strength was calibrated to be as 1.38 ± 0.01 .

KEYWORDS: Welding, welding parameters, weld joint, laser, duplex stainless steel, shear test.

1. INTRODUCTION

The duplex stainless steels (DSS) have been developed to provide a combination of high strength and resistance to corrosion. These properties are used in a variety of applications, such as chemical, structural, power plant, nuclear, transport and tanker applications, food processing and many others. Understanding the complex factors that affect the weldability of these materials is critical to the successful implementation [1–4].

Numerous experimental investigations have been performed to the laser beam welding of DSS. Laser has the potential to accelerate the fabrication of components, however, some metallurgical challenges limit its applications in DSS. Solidification is fully ferritic and followed by the diffusion-controlled solid-state ferrite to austenite transformation. Rapid cooling, when using laser welding, restricts austenite formation and disturbs the optimum phase balance in DSS. The ferrite/austenite balance has an influence on mechanical and corrosion properties. Optimal properties of DSS are obtained at about 50% ratio of austenite and ferrite in the microstructure. Consequently, it is expected that the ferrite/austenite balance in fusion zone (FZ) is affected by heat input of laser beam. The heat input is mainly affected by welding parameters such as laser beam power, welding speed and focal position [1–11].

Other ways that affect the ferrite/austenite ratio at laser beam welding are using of nitrogen as shielding gas and using of laser reheating. Both leads to the increasing of austenite contents in FZ and heat affected zone (HAZ). The effect of nitrogen and reheating has been characterized in terms of tensile properties, fractography, hardness and corrosion resistance [1–5].

Some investigations have been devoted to using a multi-beam laser welding process. The numerical analysis of the laser welding process using a dual beam have been applied to perform reheating with a second laser beam to achieve appropriate ferrite/austenite ratio [12, 13].

The present study is concerned with dual beam laser welding and its effect on size and microstructure of FZ and mechanical properties of DSS weld joints. Tensile tests of weld joints lead to fractures in base metal, so the strength properties were assessed by applying a shear strength test right in the FZ of weld joints [14].

2. MATERIALS AND METHODS

The welded materials are a commercial DSS EN 1.4362 (DSS 2304) and EN 1.4410 (DSS 2507). Chemical compositions of materials are shown in Table 1.

Dissimilar sheets of DSS 2507–DSS 2304 were welded in butt joint configuration. Specimen dimensions were 140×100 mm, thickness 5 mm. An indus-

wt.%	C	Mn	P	S	Si	Cr	Ni	Mo	N	Cu
DSS 2304	≤ 0.03	≤ 2	≤ 0.035	≤ 0.015	≤ 1.0	22.5	4.5	0.3	0.1	0.3
DSS 2507	≤ 0.03	≤ 1.2	≤ 0.025	≤ 0.015	≤ 0.8	25	7	4	0.3	0

TABLE 1. Chemical composition of materials EN 1.4362 (DSS 2304), EN 1.4410 (DSS 2507).

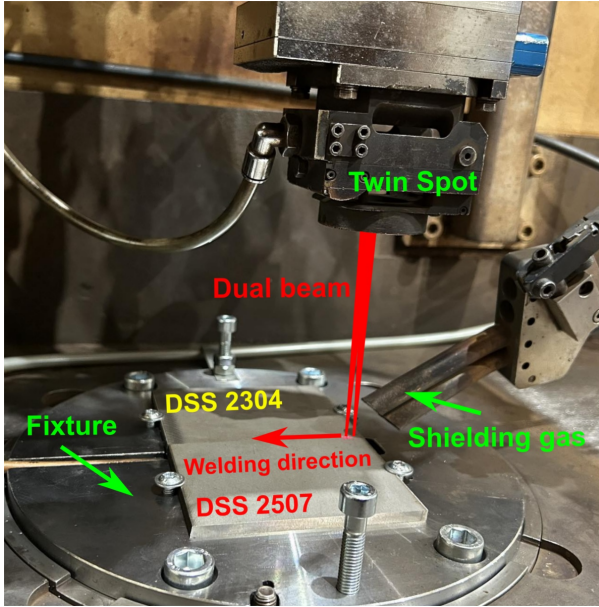
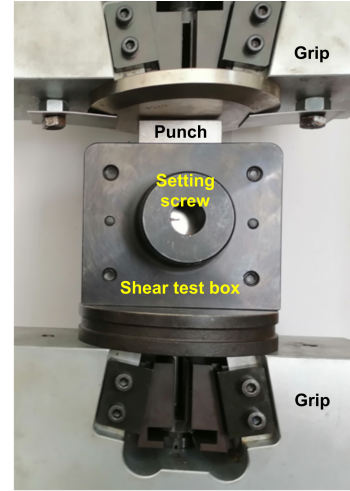


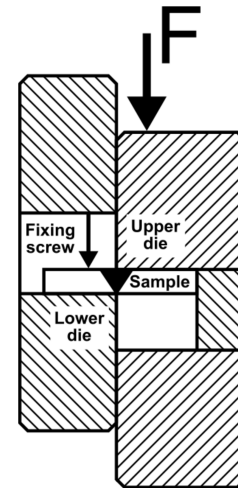
FIGURE 1. Arrangement of welding.

trial fiber laser type IPG YLS 5000 with a wavelength of $1.06 \mu\text{m}$ and a maximum output power of 5 kW was used to weld dissimilar joints. The Precitec YW52 laser head was supplemented with a special twin-spot module (Figure 1), which enables the splitting of the laser beam. Beam power ratios (primary beam: secondary beam) of 50:50, 65:35 and 80:20 was used. The dual beam was applied in a tandem configuration with a distance of 1.7 mm between beam axes. Constant welding parameters were laser beam power 3400 W, welding speed 10 mm s^{-1} , focal position 0 mm. Argon was selected as the shielding gas and a flow rate on the surface was 25 l min^{-1} . Beam power ratio were changed on 50:50 (sample 50:50), 65:35 (sample 65:35) and 80:20 (sample 80:20).

Samples of weld joints were subjected to metallographic analysis and testing of mechanical properties. At metallographic analysis FZ geometry (bead shape), resulting microstructure, ferrite/austenite ratio and microhardness HV0.1, were investigated using optical microscope Neophot 32, stereomicroscope Stemi 2000-c and ImageJ. Testing of mechanical properties such as tensile strength and shear strength were investigated using the universal testing machine Tinius Olsen 300ST. During the tensile strength test, the samples were broken at the base metal. This does not give an overview of the strength of FZ of weld joint. The strength properties were therefore assessed by applying a shear strength test equipment (Figure 2a).



(A). Shear testing equipment.



(B). Scheme of shear test.

FIGURE 2. Shear strength test.

A schematic view of the shear strength test is shown in Figure 2b.

3. RESULTS AND DISCUSSION

The weld bead shows full penetration for all the weld samples, however, the variation in weld bead shapes is observed due to changes in the dual beam power ratio. The beam power ratio 50:50 leads to the formation of a typical vine glass shaped weld bead. The front side width is 5.59 mm and the back side width is 1.10 mm (Figure 3a). Changing the power ratio on 65:35 and 80:20 leads to decreasing of the front side width to 4.04 mm and 4.19 mm respectively and increasing the back side width to 2.57 mm and 2.42 mm respectively (Figure 3b, 3c).

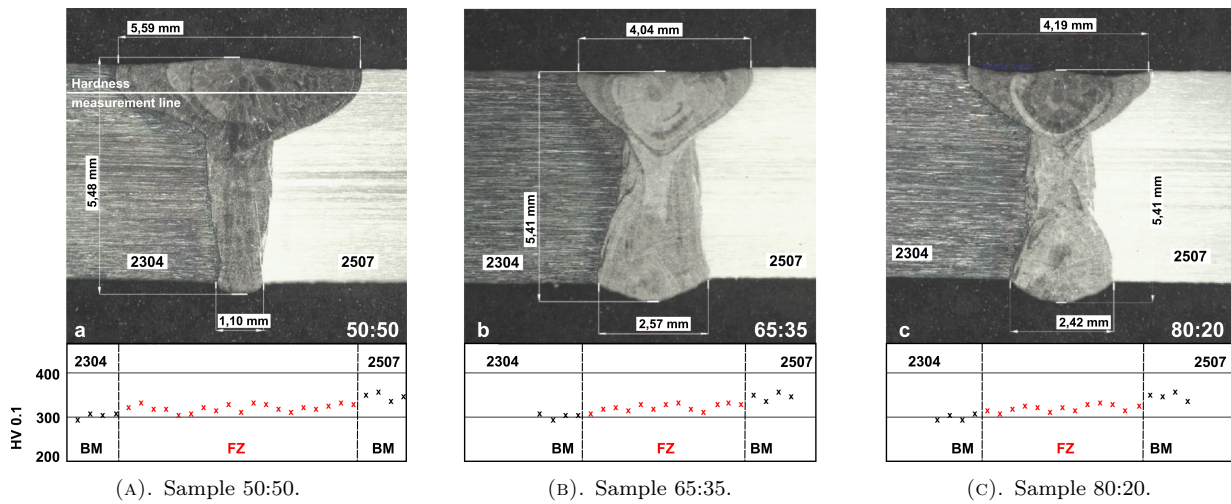


FIGURE 3. Weld bead geometry and HV0.1.

The FZ microstructure consists of the networks of austenite at the ferritic grain boundaries. The observed weld beads exhibited different content of austenite in the range from 16% to 26%. The highest content of austenite was found in sample 65:35 using dual beam power ratio 65:35. The laser beam power ratio 50:50 and 80:20 had importantly almost the same influence on ferrite/austenite ratio 84:16% and 83:17% respectively. For further increasing of austenite content, it would be necessary to use above mentioned methods: nitrogen as shielding gas, laser reheating and so on.

The microhardness HV0.1 along the weld cross-section (hardness measurement line Figure 3a) for varying dual beam power ratio was measured (Figure 3). It can be noted that the beam power ratio has no significant influence on hardness values. The highest value was measured at DSS 2507 base material (330 to 357). The microhardness of the DSS 2304 base material and FZ were in the range from 295 to 306 and from 318 to 334 respectively. So, the hardness of FZ reaches higher values in comparison with DSS 2304 base material and something lower values in comparison with DSS 2507 base material.

The tensile strength was evaluated for all the weld joints with varying dual beam power ratios (samples 50:50, 65:35 and 80:20). For each sample, three testing specimens were prepared and tested. During the tensile test all the specimens were broken in the DSS 2304 base material (Figure 4) and the reached values are in the range from 777 to 783 MPa.

If there is a fracture in the base material, the weld joint is evaluated as satisfactory, but there is no information about the strength of FZ and HAZ. So, the strength properties were assessed by applying the shear strength test right in the FZ of the weld joints. For each sample (50:50, 65:35 and 80:20) two testing specimens were prepared and tested. The specimens after shear strength test are shown in Figure 5.



FIGURE 4. Specimens after tensile strength test.



FIGURE 5. Specimens after shear strength test.

Typical sheared edge of FZ for specimen 65:35 is shown in Figure 6. The sheared edge consists of a burnish zone and a fracture zone. In the front side of the weld bead deformed rollover zone can be seen. The shear test was conducted using 0.1 mm shearing clearance.

The load-displacement diagrams created during shear strength test for the FZ (specimens 50:50, 65:35 and 80:20) are shown in Figure 7. The diagrams have almost the same course, nevertheless, some differences in the maximum load can be seen (50:50 – 24500 N, 65:35 – 23800 N and 80:20 – 24100 N). This was reflected in the calculated strength values of the tested specimens. The decrease in the load value corresponds to the increase in the austenite content in the fusion zone.

The shear strength for FZ of samples 50:50 reached values 641 and 649 MPa, for sample 65:35 reached 625 and 629 MPa and for sample 80:20 reached 630 and 638 MPa. To compare and to determine the propor-

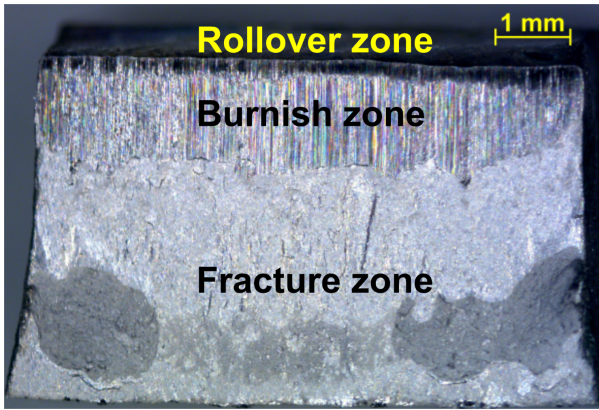


FIGURE 6. Sheared edge of FZ (specimen 65:35).

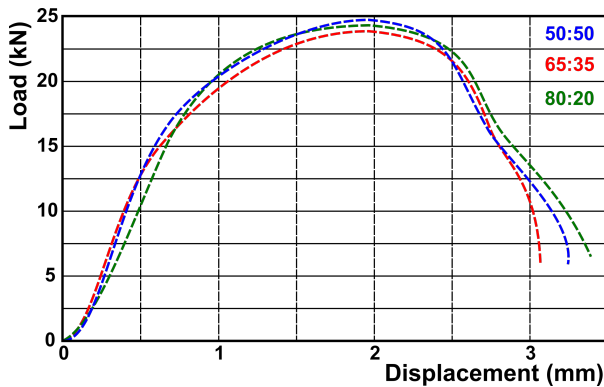


FIGURE 7. Shear strength test diagrams.

tionality coefficient between tensile strength and shear strength, the shear strength test was also carried out for both DSS 2304 and DSS 2507 base materials. From the values of tensile strength R_m and shear strength R_{ms} of the DSS 2304 base material, the proportionality coefficient “ k ” can be calculated. The value of “ k ” = R_m/R_{ms} = $780 \pm 3 \text{ MPa} / 565 \pm 2 \text{ MPa} \doteq 1.38 \pm 0.01$. Using this coefficient the proportional tensile strength of DSS 2507 base material and FZ of weld joints were calculated. Measured and calculated strength characteristics are given in Table 2.

Sample	Tensile test Strength [MPa]	Shear test Strength [MPa]
BM DSS 2304	780 ± 3	565 ± 2
BM DSS 2507	$\doteq 861 \pm 9^*$	624 ± 2
FZ 50:50	$\doteq 890 \pm 12^*$	645 ± 4
FZ 65:35	$\doteq 865 \pm 9^*$	627 ± 2
FZ 80:20	$\doteq 875 \pm 12^*$	634 ± 4

* Calculated tensile strength using “ k ” $\doteq 1.38 \pm 0.01$

TABLE 2. Measured and calculated strength characteristics.

4. CONCLUSIONS

The use of the dual beam with different values of beam power ratios leads to significant changes in the bead

shape, especially the front side width and back side width were changed.

The investigated FZ exhibited different content of austenite in the range from 16 % to 26 %. The highest content of austenite was found in sample 65:35, when the laser beam power ratio was 65:35. This also leads to decreasing of the shear strength of the FZ.

Measurement of hardness did not reveal any significant differences of values for all measured weld joints, so the dual beam power ratio influence on hardness is negligible.

The fracture location at the tensile test was in the base material for all specimens, so the weld joint tensile strength is satisfactory but no information was obtained about the strength of FZ. Therefore, the shear strength test was applied. The shear strength of both base materials and all FZ samples was measured. The coefficient of proportionality between shear strength and tensile strength was calibrated to be as 1.38 ± 0.01 . The highest value of the shear strength (649 MPa) was measured for the FZ of sample 50:50.

The weld joint prepared according to the above-mentioned parameters exhibited the full penetration and defects free FZ. The mechanical properties of the FZ are satisfactory, however the content of austenite in microstructure is still unbalanced.

ACKNOWLEDGEMENTS

This work was supported by the Slovak Research and Development Agency under the contract No. APVV-21-0232.

REFERENCES

- [1] A.-M. El-Batahgy, A.-F. Khourshid, T. Sharef. Effect of laser beam welding parameters on microstructure and properties of duplex stainless steel. *Materials Sciences and Applications* **2**(10):1443–1451, 2011. <https://doi.org/10.4236/msa.2011.210195>
- [2] H. S. Abdo, A. H. Seikh. Mechanical properties and microstructural characterization of laser welded S32520 duplex stainless steel. *Materials* **14**(19):5532, 2021. <https://doi.org/10.3390/ma14195532>
- [3] G. N. Ahmad, N. K. Singh, B. N. Tripathi, et al. Monitoring of thermo-cycles in fibre laser welding of duplex stainless steel 2205 sheets and its correlation with microstructures and mechanical properties. *Materials Research Express* **10**(10):106517, 2023. <https://doi.org/10.1088/2053-1591/ad0095>
- [4] A. Baghdadchi, V. A. Hosseini, K. Hurtig, L. Karlsson. Promoting austenite formation in laser welding of duplex stainless steel – impact of shielding gas and laser reheating. *Welding in the World* **65**:499–511, 2021. <https://doi.org/10.1007/s40194-020-01026-7>
- [5] W. W. Zhang, S. Cong, S. B. Luo, J. H. Fang. Effects of energy density and shielding medium on performance of laser beam welding (LBW) joints on SAF2205 duplex stainless steel. *The Journal of The Minerals, Metals & Materials Society* **70**:1554–1559, 2018. <https://doi.org/10.1007/s11837-018-2872-6>

- [6] M. Bolut, C. Y. Kong, J. Blackburn, et al. Yb-fibre laser welding of 6 mm duplex stainless steel 2205. *Physics Procedia* **83**:417–425, 2016. <https://doi.org/10.1016/j.phpro.2016.08.043>
- [7] E. R. Fábián, J. Dobránszky, J. Csizmazia, R. Ott. Effect of laser beam welding on the microstructure of duplex stainless steels. *Materials Science Forum* **885**:245–250, 2017. <https://doi.org/10.4028/www.scientific.net/MSF.885.245>
- [8] A. Ghosh, D. Misra, S. K. Acharyya. Experimental and numerical investigation on laser welding of 2205 duplex stainless steel. *Lasers in Manufacturing and Materials Processing* **6**:228–246, 2019. <https://doi.org/10.1007/s40516-019-00090-2>
- [9] M. Landowski, S. C. Simon, C. Breznay, et al. Effects of preheating on laser beam-welded NSSC 2120 lean duplex steel. *The International Journal of Advanced Manufacturing Technology* **130**:2009–2021, 2024. <https://doi.org/10.1007/s00170-023-12840-w>
- [10] R. Sołtysiak, T. Giętka, A. Sołtysiak. The effect of laser welding power on the properties of the joint made of 1.4462 duplex stainless steel. *Advances in Mechanical Engineering* **10**(1):1687814017751949, 2018. <https://doi.org/10.1177/1687814017751949>
- [11] S. Zhao, Y. Bi. Influence of heat input on microstructure and mechanical properties of laser weld metal in 2507 duplex stainless steel by different welding speed and welding power. *Materials Science* **30**(1):26–33, 2024. <https://doi.org/10.5755/j02.ms.34338>
- [12] A. Fey, S. Ulrich, S. Jahn, P. Schaaf. Numerical analysis of temperature distribution during laser deep welding of duplex stainless steel using a two-beam method. *Welding in the World* **64**:623–632, 2020. <https://doi.org/10.1007/s40194-020-00857-8>
- [13] S. M. Robertson, A. F. H. Kaplan. Multi-keyhole separation during multi-spot laser welding of duplex steel. *Optics & Laser Technology* **143**:107382, 2021. <https://doi.org/10.1016/j.optlastec.2021.107382>
- [14] M. Martinkovič, P. Kovačócy. Possibilities of analyzing the mechanical properties of welded and soldered joints. *Journal of Physics: Conference Series* **2712**(1):012023, 2024. <https://doi.org/10.1088/1742-6596/2712/1/012023>